LETTERS

Auxin inhibits endocytosis and promotes its own efflux from cells

Tomasz Paciorek[1], Eva Zažímalová[2], Nadia Ruthardt[3], Jan Petrášek[2], York-Dieter Stierhof[1], Jürgen Kleine-Vehn[1], David A. Morris[2,4], Neil Emans[3], Gerd Jürgens[1], Niko Geldner[1] & Jiří Friml[1]

One of the mechanisms by which signalling molecules regulate cellular behaviour is modulating subcellular protein translocation. This mode of regulation is often based on specialized vesicle trafficking, termed constitutive cycling, which consists of repeated internalization and recycling of proteins to and from the plasma membrane[1]. No such mechanism of hormone action has been shown in plants although several proteins, including the PIN auxin efflux facilitators, exhibit constitutive cycling[2,3]. Here we show that a major regulator of plant development, auxin, inhibits endocytosis. This effect is specific to biologically active auxins and requires activity of the Calossin-like protein BIG. By inhibiting the internalization step of PIN constitutive cycling, auxin increases levels of PINs at the plasma membrane. Concomitantly, auxin promotes its own efflux from cells by a vesicle-trafficking-dependent mechanism. Furthermore, asymmetric auxin translocation during gravitropism is correlated with decreased PIN internalization. Our data imply a previously undescribed mode of plant hormone action: by modulating PIN protein trafficking, auxin regulates PIN abundance and activity at the cell surface, providing a mechanism for the feedback regulation of auxin transport.

The local, asymmetric distribution of the plant growth regulator auxin mediates a variety of developmental processes such as axis formation, organ initiation and positioning, directional growth (tropisms) and meristem activity[4–6]. Biochemical, genetic and molecular data have confirmed that auxin promotes SCF^{TIR1}-mediated ubiquitination and degradation of the auxin/indole-3-acetic acid (AUX/IAA) repressors, thus releasing auxin response factor (ARF) transcriptional regulators from inhibition[7]. In this manner the expression of different sets of genes is activated, thereby eliciting different cellular and, consequently, developmental responses. An important additional level of regulation upstream of cellular auxin signalling is a specific transport system dependent on polarly localized PIN auxin efflux regulators[8]. This dynamic auxin distribution network mediates directional (polar) auxin flow between cells, which contributes to the formation and maintenance of asymmetric auxin distribution.

PIN proteins rapidly and constitutively cycle between the plasma membrane (PM) and endosomes[2]. In *Arabidopsis* this cycling involves a brefeldin A (BFA)-sensitive regulator of vesicle budding, the guanosine exchange factor for adenosine-ribosylation-factor-type small GTPases (ARF GEF) known as GNOM[3]. BFA inhibits trafficking from endosomes to the PM and causes endosomes to aggregate into 'BFA compartments'[2], which become surrounded by Golgi stacks[3]. In contrast, trafficking from the PM to the endosomes seems to be insensitive to BFA. These differential effects of BFA on endocytosis and exocytosis lead to the internalization and accumulation of constitutively cycling proteins in the BFA compartments. Thus, in *Arabidopsis* BFA can serve as a tool for revealing subcellular protein movement between endosomes and the PM[2,3].

Several plant PM markers were rapidly and reversibly internalized in response to BFA. These included PIN auxin efflux regulators such as PIN1 (ref. 2) (Fig. 1a, b), PIN2 (ref. 3) (Supplementary Fig. S1a), PIN3 (ref. 4) and PIN4 (Supplementary Fig. S1d), the PM water channel PIP2 (Fig. 1d) and maize cell-wall pectins[9] (Supplementary Figure S1h). Plasma membrane H^+-ATPase (PM-ATPase) was preferentially internalized in rapidly elongating epidermal cells (Fig. 1c), indicating the possible existence of both dynamic and more static populations of the protein. BFA-induced reversible internalization also occurred when transcription, protein synthesis[2] or protein degradation were inhibited (Supplementary Fig. S2), confirming that proteins accumulating in BFA compartments were not synthesized *de novo* but originated from the PM. Co-localization of cycling proteins (Supplementary Fig. S1a–c), the endocytic tracer FM4-64 (Supplementary Fig. S1e–g) and endosomal markers (Fig. 2b) revealed that the proteins studied here recycle through the same endomembrane compartments. These data show that some plant PM proteins are retained at the PM, but many exhibit constitutive cycling between the PM and endosomes.

In animals, constitutive cycling is an entry point for multiple regulation, including by signalling molecules[1]. Through this mechanism, hormones such as insulin or vasopressin can control the relative rates of endocytosis and exocytosis and thereby regulate the concentrations, and thus the activity of surface-localized proteins, including ion and water channels, transporters and receptors[1]. In plants, even high concentrations of several phytohormones including abscisic acid, brassinosteroids, cytokinins, ethylene and gibberellins had no detectable effect on various trafficking processes, including BFA-induced internalization (Fig. 1h, Supplementary Fig. S3). Interestingly, however, auxins such as the naturally occurring IAA and its synthetic analogues naphthalene-1-acetic acid (NAA) and 2,4-dichlorophenoxyacetic acid (2,4-D) efficiently inhibited the internalization of PIN1, PIN2, PIN4, PM-ATPase, PIP2:GFP and maize cell wall pectins in response to BFA (Fig. 1e–g, Supplementary Fig. S1i–p). Concentrations as low as 5 μM NAA and 2,4-D were enough to elicit near-maximal effects (Fig. 1e, f, Supplementary Fig. S4) indicating that these compounds might be sufficiently active even at lower concentrations. IAA was chemically unstable under our experimental conditions (verified by high-performance liquid chromatography and mass spectroscopy; Supplementary Fig. S5), but when an antioxidant (butylated hydroxytoluene; BHT[10]) was included in the medium, IAA was also effective at concentrations as low as 5 μM (Fig. 1g, Supplementary Fig. S5). In contrast, the physiologically inactive structural isomer of

[1]Zentrum für Molekularbiologie der Pflanzen, Universität Tübingen, 72076 Tübingen, Germany. [2]Institute of Experimental Botany, ASCR, Rozvojová 135, 165 02 Praha 6, Czech Republic. [3]Cellome Research Group, RWTH Aachen University, Biology VII, Worringerweg 1, 52074 Aachen, Germany. [4]School of Biological Sciences, University of Southampton, Bassett Crescent East, Southampton SO16 7PX, UK.

NAA, naphthalene-2-acetic acid (2-NAA), had no effect even at a tenfold higher concentration (Fig. 1i). However, even at maximal effective concentrations, auxins did not completely block BFA-induced internalization. This is inferred from the observation that some accumulation of constitutively cycling PM proteins inside cells could be observed when the treatment with BFA in the presence of auxins was prolonged (Supplementary Fig. S6).

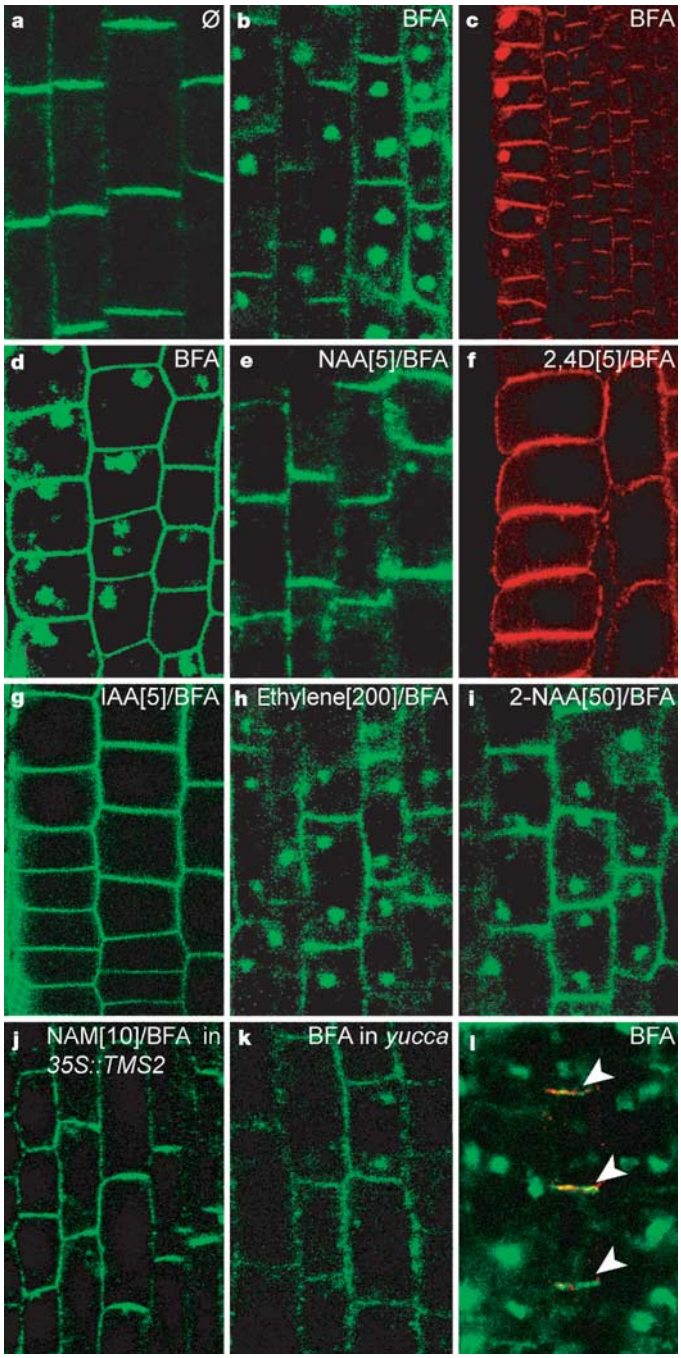

Figure 1 | Auxins inhibit internalization of constitutively cycling proteins. **a**–**d**, BFA-induced internalization of PM proteins: Polar, PM localization of PIN1 in untreated (∅) roots (**a**); PIN1 (**b**) and PIP2:GFP (**d**) internalization. BFA-sensitive (epidermis, cortex) and BFA-insensitive (stele) pools of PM-ATPase (**c**). **e**–**g**, Auxins (NAA, 2,4-D and IAA) inhibit BFA-induced internalization of PIN1 (**e**), PM-ATPase (**f**) and PIP2:GFP (**g**). **h**, **i**, Other hormones including ethylene (aminocyclopropane carboxylic acid (**h**)) or the inactive NAA analogue 2-NAA (**i**) are ineffective. **j**, NAA amide (NAM) in *35S::TMS2* plants inhibits BFA-induced internalization. **k**, *yucca* mutants show decreased PIN1 internalization. **l**, Protophloem cells marked by AUX1 (red) show less BFA-induced PIN1 (green) internalization than surrounding cells. Numbers in square brackets are concentrations in μM.

Induced increases in intracellular concentrations of endogenous auxin also had an inhibitory effect on the internalization of constitutively cycling PM proteins. *35S::TMS2* plants overexpress the amidohydrolase that converts biologically inactive auxin amides into active auxins[11]. When treated with NAA amide or IAA amide, *35S::TMS2* (Fig. 1j) but not wild-type plants (data not shown) showed inhibition of BFA-induced PIN1 internalization. Furthermore, *Arabidopsis* mutants with increased concentrations of endogenous auxin such as *superroot1* (*sur1*)[12] (data not shown) or *yucca*[13] (Fig. 1k) showed decreased PIN1 internalization after treatment with BFA in comparison with wild-type plants. Protophloem cells of root have been shown to have higher concentrations of auxin than surrounding tissues[14]. In wild-type plants grown under normal conditions, BFA-induced internalization was clearly inhibited in these cells (Fig. 1l). Together, these results show that physiological concentrations of exogenously applied and/or endogenously produced auxins downregulate the BFA-induced internalization of constitutively cycling PM proteins.

Next we examined the subcellular site(s) at which auxin acts on the BFA-induced internalization of PM proteins. An important control was the confirmation that auxins did not influence the uptake of BFA into *Arabidopsis* roots (Supplementary Fig. S7). To assess possible effects of auxin on different trafficking processes, we used established markers for various endomembrane compartments. There were no apparent effects of auxin on the distribution of ER (Sec12 (ref. 3)), presumptive trans-Golgi network (TLG2a (ref. 3)), Golgi apparatus (γ-COP (ref. 3)) or endosomal (ARF1 (ref. 15)) markers (Supplementary Fig. S8). Auxins also did not interfere with the BFA-induced formation of endosomal BFA compartments or with the aggregation of Golgi stacks at their periphery (Fig. 2a–f, Supplementary Fig. S9). Double labelling revealed that, in the same cells, auxin treatment did not affect the formation of Golgi-stack-encircled BFA compartments but prevented the internalization of PM proteins and therefore their accumulation in such compartments (Fig. 2c, f). The observation that BFA compartments (revealed as an aggregation of endocytic vesicles) still formed after treatment with auxin was confirmed by an examination of ultrastructure by electron microscopy (Fig. 2k–m). These data indicate that auxins might interfere with the endocytic step of constitutive cycling without visibly affecting other subcellular trafficking processes.

To assess directly the effect of auxin on endocytosis, we used the fluorescent dye FM4-64, an established endocytic tracer[3]. In *Arabidopsis* roots, even low concentrations of exogenously applied auxins clearly decreased the detectable uptake of FM4-64 (Fig. 2g, h), showing the inhibition of endocytosis. Furthermore, in *yucca* roots, which contain higher concentrations of endogenous IAA[13], the uptake of FM4-64 was also inhibited (Fig. 2i). To confirm and quantify the auxin effect on endocytosis, we measured the uptake of another endocytic tracer, FM1-43 (ref. 16), into suspension-grown tobacco BY-2 cells. Both 2,4-D and NAA inhibited FM1-43 uptake in a concentration-dependent manner (Fig. 2j). NAA was less effective, which is consistent with its decreased retention in tobacco cells[17]. Auxins also completely abolished the BFA-induced increase in FM1-43 internalization that results from the inhibition of membrane recycling back to the cell surface[16]. These experiments confirmed that the endocytic step of the cycling of PM proteins is the target for auxin action.

For a molecular characterization of the pathway by which auxin inhibits endocytosis, we performed a genetic screen to find mutants altered in the auxin effect on endocytosis. One group of mutants that showed resistance to the auxin effect on endocytosis was allelic to *transport inhibitor response3* (*tir3*). *tir3* was originally isolated in a screen for resistance to auxin transport inhibitors[18] and other alleles have also been identified by their involvement in light signal

transduction (*dark overexpression of CAB1* (*doc1*) and *attenuated shade avoidance* (*asa1*)) or cytokinin response (*umbrella* (*umb1*))[19,20]. The corresponding gene, since renamed *BIG*, encodes a member of the Calossin/Pushover family present in other multicellular organisms[19]. These proteins might be involved in subcellular vesicle trafficking, because they affect the subcellular localization of PIN1 after treatment with auxin efflux inhibitors[19]. We found that in both the *tir3* and *doc1* alleles of *big*, endocytosis of PM proteins was inhibited by auxins less than in the wild type. Auxin concentrations that would normally lead to the visible inhibition of BFA-induced internalization of the PIN1 protein (Fig. 3a–c) were ineffective in *big* mutants (Fig. 3e–g). Only higher auxin concentrations were able to inhibit the BFA-induced internalization (Fig. 3d, h). Other tested PM proteins such as PIN2 (data not shown) and PM-ATPase (Fig. 3i) behaved in a similar way as PIN1. Furthermore, *big* mutants also showed resistance to endogenously increased auxin concentrations in combination with *yucca* mutants, as demonstrated by a pronounced inhibition of BFA-induced internalization in *yucca* (see Fig. 1k), but not in *yucca big*, mutant roots (Fig. 3j). In addition, the inhibitory effect of auxin on the internalization of the endocytic tracer FM4-64 (see Fig. 2g–i) was less pronounced in *big* mutant roots (Fig. 3k). These data indicate that BIG is required for the auxin-mediated inhibition of endocytosis and thereby identify a molecular component of this specific pathway of auxin action.

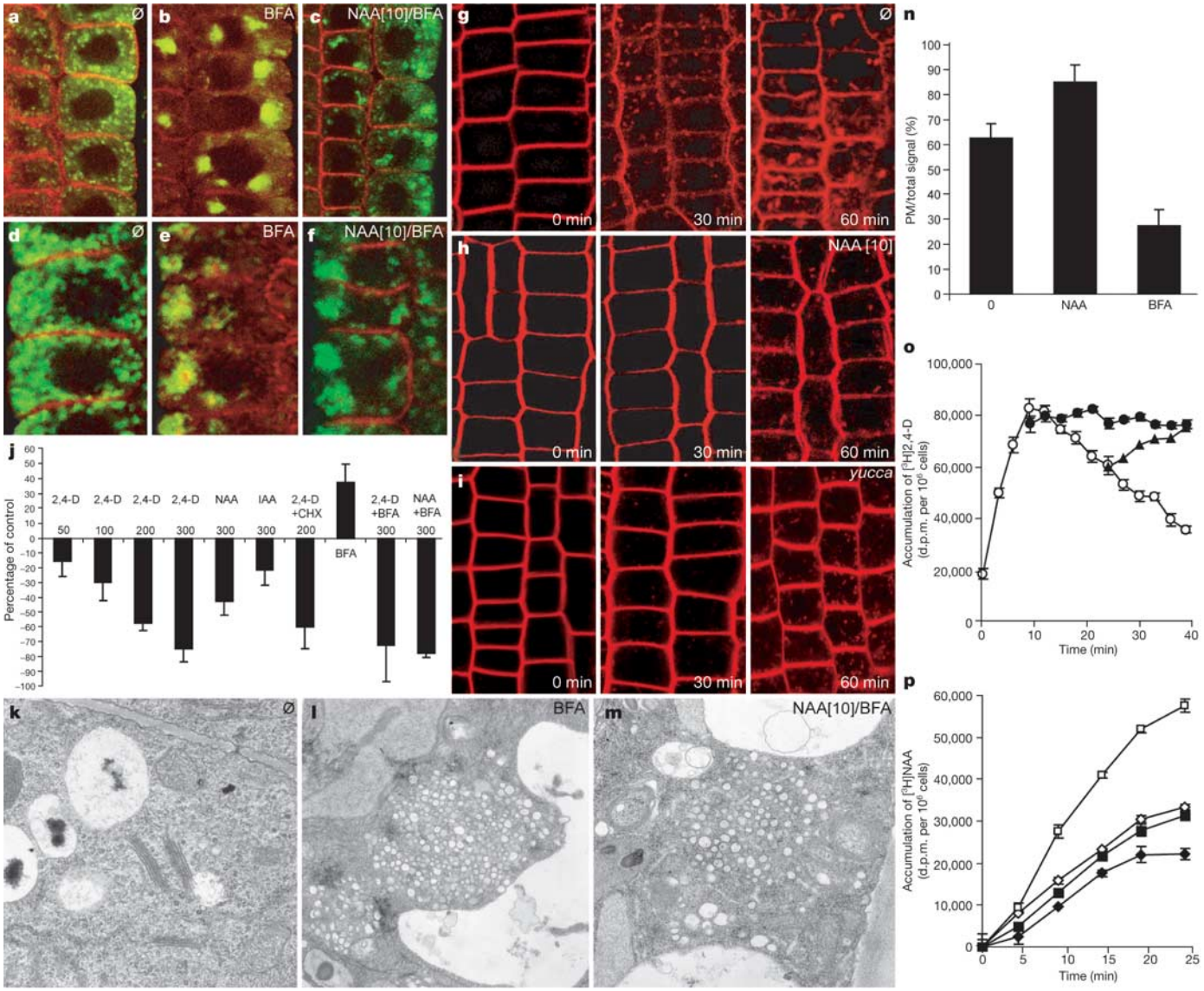

Figure 2 | Auxin inhibits endocytosis, increases the amount of PIN2 protein at the plasma membrane and stimulates its own efflux from tobacco cells. **a**–**c**, PM-ATPase (red) is internalized in response to BFA into ARF1-containing (green), endosomal BFA compartments (**b**). After treatment with NAA, PM-ATPase does not internalize, but ARF1-containing endosomes aggregate (**c**). **d**–**f**, γ-COP-labelled Golgi apparatus (green) aggregates around PM-ATPase-containing BFA compartments (red) (**e**). NAA prevents PM-ATPase internalization but not γ-COP aggregation (**f**). **g**–**i**, Uptake of endocytic tracer FM4-64 is slowed down in NAA-treated roots (**h**) and in *yucca* roots (**i**). **j**, 2,4-D, NAA and IAA inhibit uptake of FM1-43 into BY-2 cells in a concentration-dependent manner. Concentrations shown are in μM. CHX, cycloheximide. **k**–**m**, Ultrastructural examination of BFA compartments did not reveal any differences in ultrastructure between BFA (**l**) and NAA/BFA (**m**) treatments. **n**, The ratio of PM-located to internalized PIN2 signals (in %) increases after NAA and decreases after BFA treatments. **o**, [^{3}H]2,4-D decreases its own accumulation in VBI-0 cells over time (open circles). Concomitant BFA treatment (applied 6 min after addition of [^{3}H]2,4-D) prevents this effect (filled circles), and NAA (applied 21 min after addition of [^{3}H]2,4-D) competitively inhibits [^{3}H]2,4-D export (triangles). **p**, Pretreatment with 2,4-D for 20 min (filled diamonds) decreases [^{3}H]NAA accumulation in the BY-2 cells. BFA increases the accumulation (open squares), but this effect is prevented by pretreatment with 2,4-D (filled squares). Open diamonds, no addition. **a**, **d**, **g**, **k**, Untreated controls. Numbers in square brackets are concentrations in μM. Error bars show s.d.; ∅ relates to untreated controls.

If auxins inhibit the endocytic step of constitutive cycling, the protein pool at the PM should increase after treatment with auxin. To test this prediction we directly measured the ratio of cell surface to internalized PIN2 protein by using quantitative confocal microscopy. In the control (no auxin treatment), the PM pool composed approximately 62% of the total PIN2 protein. Treatment with auxins (NAA) increased the cell-surface signal significantly (85%, $P < 0.001$), showing higher levels of PIN2 at the PM (Fig. 2n). By contrast, treatment with BFA (inhibiting the exocytic step of the cycling) had the opposite effect and caused a massive accumulation of PIN2 inside cells, decreasing the cell-surface signal (28%, $P < 0.001$). Taken together, these data strongly indicate that auxins might inhibit the endocytic step of constitutively cycling PIN proteins, thus increasing their levels at the PM.

An auxin-dependent increase in the amount of cell-surface-localized PIN auxin efflux regulators would afford a mechanism by which auxin can control its own transport. A classical model, which attempts to explain multiple self-organizing auxin effects—the so-called canalization hypothesis—proposed feedback regulation between auxin signalling and intercellular auxin transport[21]. Earlier physiological experiments did indeed imply that auxin is required to maintain its own polar transport[22]. However, a direct effect of auxin on its own efflux has not been shown. The effects of auxin on its own transport were quantitatively assessed in suspension-grown tobacco cell lines VBI-0 and BY-2, which are well-established systems for studies of auxin transport *in vivo*[23,24]. The lines differ in their abilities to export different auxins, and the most important feature related to this study is that 2,4-D is a much better substrate for an auxin efflux machinery in VBI-0 cells than in BY-2 cells (Supplementary Fig. S10a–c). Generally, the net accumulation of radioactively labelled auxins in cells gives a measure of the relative rates of their uptake and efflux. In constant carrier-driven (and thus saturable) transport across the PM, the auxin accumulation would be expected to exhibit saturation kinetics until the uptake and efflux rates reached equilibrium. When VBI-0 cells were incubated with [^{3}H]2,4-D, after an initial increase in its internal concentration, the accumulation of [^{3}H]2,4-D decreased steadily with time instead of reaching a stable equilibrium (Fig. 2o). This effect was completely reversed by both a known inhibitor of auxin efflux (1-naphthylphthalamic acid (NPA); Supplementary Fig. S10d) and a high-affinity substrate for efflux carrier(s) in tobacco cells (NAA[17,23]; Fig. 2o). This shows that the observed decrease in 2,4-D accumulation results from an increased capacity in its carrier-driven efflux. This decrease in accumulation

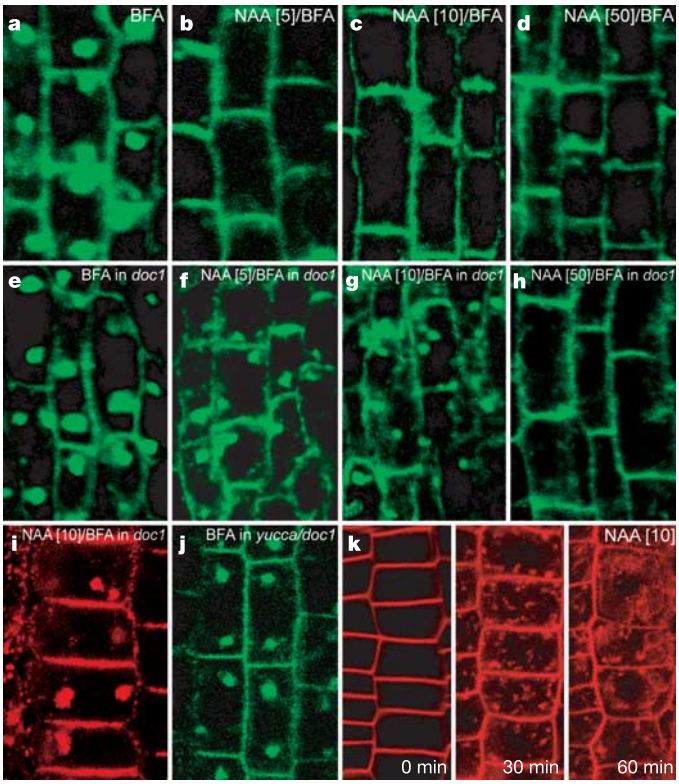

Figure 3 | BIG protein is required for the auxin-dependent inhibition of endocytosis. **a**–**h**, *doc1* mutants are partly auxin-resistant: BFA causes PIN1 internalization in control (**a**) and *doc1* roots (**e**). NAA blocks PIN1 internalization in controls (**b**, **c**) but not in *doc1* (**f**, **g**). Higher NAA concentrations are effective in both control (**d**) and *doc1* (**h**). **i**, In *doc1*, BFA-induced internalization of PM-ATPase is resistant to auxin (compare with Fig. 1f). **j**, Increase in auxin concentrations in *yucca* does not inhibit PIN1 internalization in the *yucca doc1* double mutant (compare with Fig. 1k). **k**, NAA does not inhibit the uptake of FM4-64 in the *doc1* mutant (compare with Fig. 2g, h). Numbers in square brackets are concentrations in μM.

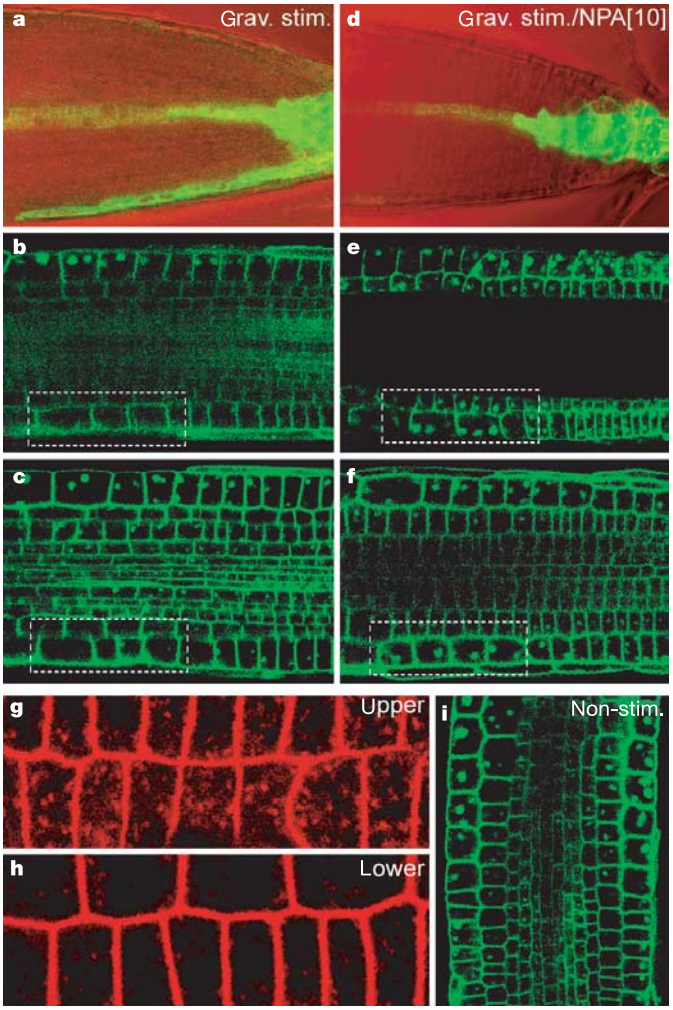

Figure 4 | Correlation between auxin translocation and the rate of PIN2 internalization in course of root gravitropism. **a**–**c**, After stimulation by gravity, auxin translocation detected by DR5rev::GFP activity (**a**) at the lower side of roots is correlated with the inhibition of BFA-induced internalization of PIN2:GFP (**b**) and PIP2:GFP (**c**). **d**–**f**, When auxin translocation is prevented by NPA, no asymmetry in DR5rev::GFP expression (**d**) or BFA-induced internalization of PIN2:GFP (**e**) and PIP2:GFP (**f**) occurs. **g**, **h**, After stimulation by gravity, FM4-64 uptake is lower in layers on the underside of the root (**h**) than in those on the upper side (**g**). **i**, Without stimulation by gravity, no asymmetry in the BFA-induced internalization of PIP2:GFP was detected. Numbers in square brackets are concentrations in μM.

(that is, an increase in efflux) was abolished by treatment with BFA (Fig. 2o), indicating that the stimulation of 2,4-D efflux was dependent on BFA-sensitive recycling of auxin efflux carriers back to PM. Next we investigated whether the pretreatment with auxin could directly affect the activity of auxin efflux. In this case, the accumulation of auxin had to be measured by using an auxin that is taken up by passive diffusion (to exclude the possible interference by the activity of auxin influx carriers) and, simultaneously, one that is a good substrate for efflux carrier(s) in tobacco cells; NAA fulfilled these criteria in both VBI-0 and BY-2 cells. In contrast, for the pretreatment, an auxin that is a weak substrate for an auxin efflux carrier had to be used to prevent competitive inhibition of NAA efflux. Because in VBI-0 cells, but not in BY-2 cells, 2,4-D is a good substrate for an efflux carrier (Supplementary Fig. S10a–c), we used BY-2 cells for this experiment. Pretreatment for 20 min with 5 μM 2,4-D significantly decreased the accumulation of [^{3}H]NAA (increased its efflux) and, moreover, abolished the inhibitory effect of BFA on auxin efflux (Fig. 2p). Together, these data show that in tobacco cells *in vivo*, auxin stimulates its own efflux by a vesicle-trafficking-dependent mechanism. All the results are consistent with the notion that auxin inhibits the internalization of constitutively cycling auxin efflux catalysts, thus increasing their incidence at the cell surface and thereby stimulating its own efflux.

We next explored *in planta* the link between the effects of auxin on endocytosis and auxin transport. Root gravitropism—the directional growth of roots along a gravity vector—is a well-characterized physiological process that involves the rapid establishment of auxin flow along the lower side of a horizontal root after gravity perception[4,8]. This process represents an ideal system in which to examine auxin translocation and endocytic recycling in parallel. After stimulation by gravity, asymmetric auxin flow resulted in auxin accumulation at the lower side of the root, as detected by the auxin response reporter DR5rev::GFP (Fig. 4a). Significantly, a similar spatial asymmetry within the root was observed for the BFA-induced internalization of PIN2:GFP and PIP2:GFP (Fig. 4b, c), indicating that their endocytic recycling might have been inhibited at the lower side of the gravistimulated root. Reduced uptake of the endocytic tracer FM4-64 was also observed at the lower side, in comparison with the upper side, of the root (Fig. 4g, h). In contrast, no asymmetry in auxin accumulation (as detected by DR5rev::GFP; Fig. 4d) and no inhibition of PM protein internalization in response to BFA occurred in non-stimulated roots (Fig. 4i) or after treatment with NPA (Fig. 4e, f), which under these conditions inhibits auxin flow but not protein cycling[2]. Thus, asymmetric auxin translocation is closely correlated spatially with the inhibition of endocytosis during the root gravitropic response. This finding strengthens the likelihood that the effects of auxin on endocytosis and on auxin transport are linked.

Our findings indicate a previously undescribed mode of action of plant hormones, namely the modulation of protein activity by regulating their intracellular trafficking. We have shown that biologically active auxins, but not their biologically inactive analogues nor other plant hormones, negatively regulate endocytosis and the internalization of constitutively cycling proteins from the PM. These auxin-induced changes in the relative rates of endocytosis and exocytosis lead to increased concentrations of PIN auxin efflux regulators at the cell surface. Concomitantly, auxins promote their own efflux by a vesicle recycling-dependent mechanism. These two previously unidentified auxin effects share similar kinetic characteristics, substrate requirements and inhibitor sensitivities. Furthermore, when assessed in parallel *in planta* during the gravitropic response, the same root cells that exhibited increased auxin translocation also displayed a decreased rate of endocytosis. Interestingly, the *sur1* mutant, which has elevated internal auxin concentrations and downregulated endocytosis, also shows increased auxin transport[25]. All these results strongly indicate that the auxin effects on endocytosis and on its own transport might be functionally linked. Thus our results show, and provide a mechanistic explanation for, a positive auxin effect on auxin transport rate.

It remains unclear which molecular pathway auxin uses to exhibit its effect on endocytosis. Mutations in the Calossin/Pushover protein BIG render endocytosis partly auxin-resistant. *BIG* is a single-copy gene present in *Arabidopsis* and other plant and animal genomes. In *Drosophila* the mutations at the corresponding locus lead to multiple defects including altered synaptic transmission and male sterility[26]; in *Arabidopsis*, *big* mutations lead to a weak physiological resistance to auxin but also affect other signalling pathways including those for ethylene, cytokinin, gibberellin or light[20]. These data do not support a direct involvement of the BIG protein in the auxin signalling pathway but rather in more general cellular processes, possibly in some aspect of endocytosis. There is no experimental support for a connection between the BIG-dependent auxin signalling pathway for inhibiting endocytosis and previously characterized SCF^{TIR1}-related auxin signalling for the regulation of gene expression. Thus it is possible that the auxin effect on endocytosis uses a previously unknown and so far molecularly uncharacterized signalling pathway that does not involve the regulation of gene expression.

METHODS

Materials and growth conditions. The following mutants and transgenic plants of *Arabidopsis thaliana* have been described previously: *AUX1:HA*[14], *GNOM-myc*[3], *PIN1:GFP*[6], *PIN2:GFP*[15], *DR5rev::GFP*[6], *doc1* (ref. 19), *sur1* (ref. 12), *tir3* (ref. 18), *yucca*[13], *yucca doc1* double mutant[19], *35S::TMS2* (ref. 11) and *EGFP-Q8* (PIP2)[27]. Experiments were performed on 4-day-old seedlings grown on vertically oriented plates containing *Arabidopsis* medium (AM; half-strength MS agar, 1% sucrose, pH 5.8). Cells of tobacco (*Nicotiana tabacum* L., lines BY-2 and VBI-0) were grown in suspension culture as described elsewhere[23,24]. Incubation of seedlings with various chemicals was performed in 24-well cell-culture plates in liquid AM medium.

Unless otherwise indicated, the following conditions were used. Pretreatments for 30 min with 5 μM NAA, 5 μM IAA plus 400 μg ml^{-1} BHT, 5 μM 2,4-D, 50 μM 2-NAA, 200 μM aminocyclopropane carboxylic acid or 10 μM NAA amide were followed by 90 min of concomitant treatment with one of the above plus 50 μM BFA. Control treatments contained an equal amount of solvent (dimethylsulphoxide or ethanol). For gravitropism experiments, plants were grown on vertically aligned plates containing a 1-mm layer of AM medium. A gravity stimulus was applied by horizontal positioning of plates; after 60 min, BFA solution was carefully added followed by incubation for 60 min. In controls, gravitational stimulation and BFA treatments were performed in the presence of 10 μM NPA. All treatments and gravity experiments were performed at least in triplicate, with a minimum of 60 roots evaluated in total in each treatment.

Genetic screen. A mutant screen to isolate plants for resistance to auxin's inhibitory effect on PM protein internalization was performed on the ethylmethane sulphonate-mutagenized PIN1:GFP[6] population. Seedlings 5 days old were treated with 30 μM NAA for 30 min, followed by 30 μM NAA and 50 μM BFA for 90 min, and the BFA-induced internalization of PIN1:GFP was analysed with an epifluorescence microscope. From about 3,500 M1 families, we identified eight lines that under these conditions showed resistance to NAA (that is, they displayed normal internalization of PIN1:GFP into BFA compartments, as could be observed in the wild type after treatment with BFA without auxin).

Immunolocalizations. Whole-mount immunofluorescence preparations[28] and antibody staining of maize tissue sections[9] were performed as described. The rabbit anti-PIN1 polyclonal antiserum was raised against amino-acid residues 288–452 of PIN1 protein and was used previously for PIN1 localization in tissue sections[6]. For whole-mount immunolocalization in roots, immunoglobulins from the crude serum were precipitated by saturated $(NH_4)_2SO_4$ solution (2:1) and dialysed against PBS. The purified fraction was diluted 1:400. The anti-PIN2 antibody was provided by C. Luschnig and was used at a dilution of 1:400. Other antibodies were diluted as follows: anti-PIN4 (1:400)[29], anti-GFP (1:300; Molecular Probes), 9E10 anti-Myc (1:600; Santa Cruz), anti-TLG2a (1:200; Rosebiotech), anti-AtSec12 (1:50; Rosebiotech), anti-ARF1 (1:1,000)[30], anti-Atγ-COP (1:1,000)[3] and anti-PM-ATPase (1:1,000)[2]. Fluorescein isothiocyanate-conjugated and CY3-conjugated anti-rabbit secondary antibodies (Dianova) were diluted 1:200 and 1:600, respectively.

Uptake and accumulation experiments. Auxin accumulation experiments in suspension-cultured VBI-0 and BY-2 cells were performed as described previously[24]. The FM1-43 uptake experiments[16] were performed with BY-2 cells equilibrated in 2,4-D-free medium for 24 h. The measured signal was

normalized to the value of control cells at 4 °C and data were expressed relative to the 26 °C control sample. Uptake experiments with FM4-64 (Molecular Probes) in *Arabidopsis* were performed in 5-day-old seedlings, using a 5-min incubation with 1:500 dilution in AM medium.

Quantitative confocal microscopy. Quantitative confocal microscopy evaluation of the PIN2 signal was performed with Leica LCS quantification software. The scans were performed with identical microscope and laser settings for all experiments. Analysed cells on scans were selected interactively from the cortex of the same root region. Cell-border-associated and internal fluorescence were quantified separately from at least 80 cells for each treatment (10 μM NAA or 50 μM BFA for 90 min). In each experiment, inhibitors of transcription (20 μM cordycepin) and/or protein synthesis (50 μM cycloheximide) were applied to exclude any effects on PIN2 expression. Statistical significance was evaluated with Student's *t*-test.

Electron microscopy. Treatments (10 μM NAA and/or 50 μM BFA for 90 min) and ultrastructure analysis of chemically fixed root sections were performed exactly as described[2].

Received 1 February; accepted 13 April 2005.

1. Royle, S. & Murrell-Lagnado, R. Constitutive cycling: a general mechanism to regulate cell surface proteins. *BioEssays* **25,** 39–46 (2003).
2. Geldner, N., Friml, J., Stierhof, Y.-D., Jürgens, G. & Palme, K. Auxin transport inhibitors block PIN1 cycling and vesicle trafficking. *Nature* **413,** 425–428 (2001).
3. Geldner, N. *et al.* The *Arabidopsis* GNOM ARF-GEF mediates endosomal recycling, auxin transport, and auxin-dependent plant growth. *Cell* **112,** 219–230 (2003).
4. Friml, J., Wisniewska, J., Benková, E., Mendgen, K. & Palme, K. Lateral relocation of auxin efflux regulator AtPIN3 mediates tropism in *Arabidopsis*. *Nature* **415,** 806–809 (2002).
5. Friml, J. *et al.* Efflux-dependent auxin gradients establish the apical-basal axis of *Arabidopsis*. *Nature* **426,** 147–153 (2003).
6. Benková, E. *et al.* Local, efflux-dependent auxin gradients as a common module for plant organ formation. *Cell* **115,** 591–602 (2003).
7. Gray, W. R., Kepinski, S., Rouse, D., Leyser, O. & Estelle, M. Auxin regulates SCF^{TIR1}-dependent degradation of AUX/IAA proteins. *Nature* **414,** 271–276 (2001).
8. Friml, J. Auxin transport—shaping the plant. *Curr. Opin. Plant Biol.* **6,** 7–12 (2003).
9. Baluška, F. *et al.* F-actin-dependent endocytosis of cell wall pectins in meristematic root cells. Insights from brefeldin A-induced compartments. *Plant Physiol.* **130,** 422–431 (2002).
10. Von Gadow, A., Joubert, E. & Hansmann, C. F. Comparison of the antioxidant activity of aspalathin with that of other plant phenols of rooibos tea (*Aspalathus linearis*), alpha-tocopherol, BHT, and BHA. *J. Agric. Food Chem.* **45,** 632–638 (1997).
11. Karlin-Neumann, G., Brusslan, J. & Tobin, E. Phytochrome control of the *tms2* gene in transgenic *Arabidopsis*: a strategy for selecting mutants in the signal transduction pathway. *Plant Cell* **3,** 573–582 (1991).
12. Boerjan, W. *et al.* Superroot, a recessive mutation in *Arabidopsis*, confers auxin overproduction. *Plant Cell* **7,** 1405–1419 (1995).
13. Zhao, Y. *et al.* A role for flavin monooxygenase-like enzymes in auxin biosynthesis. *Science* **291,** 306–309 (2001).
14. Swarup, R. *et al.* Localisation of the auxin permease AUX1 suggests two functionally distinct hormone transport pathways operate in the *Arabidopsis* root apex. *Genes Dev.* **15,** 2648–2653 (2001).
15. Xu, J. & Scheres, B. Dissection of *Arabidopsis* ADP-RIBOSYLATION FACTOR 1 function in epidermal cell polarity. *Plant Cell* **17,** 525–536 (2005).
16. Emans, N., Zimmermann, S. & Fischer, R. Uptake of a fluorescent marker in plant cells is sensitive to brefeldin A and wortmannin. *Plant Cell* **14,** 71–86 (2002).
17. Delbarre, A., Muller, P., Imhoff, V. & Guern, J. Comparison of mechanisms controlling uptake and accumulation of 2,4-dichlorophenoxy acetic acid, naphthalene-1-acetic acid, and indole-3-acetic acid in suspension-cultured tobacco cells. *Planta* **198,** 532–541 (1996).
18. Ruegger, M. *et al.* Reduced naphthylphthalamic acid binding in the *tir3* mutant of *Arabidopsis* is associated with a reduction in polar auxin transport and diverse morphological defects. *Plant Cell* **9,** 745–757 (1997).
19. Gil, P. *et al.* BIG: a calossin-like protein required for polar auxin transport in *Arabidopsis*. *Genes Dev.* **15,** 1985–1997 (2001).
20. Kanyuka, K. *et al.* Mutations in the huge *Arabidopsis* gene BIG affect a range of hormone and light responses. *Plant J.* **35,** 57–70 (2003).
21. Berleth, T. & Sachs, T. Plant morphogenesis: long-distance coordination and local patterning. *Curr. Opin. Plant Biol.* **4,** 57–62 (2001).
22. Morris, D. A. Transmembrane auxin carrier systems—dynamic regulators of polar auxin transport. *Plant Growth Regul.* **32,** 161–172 (2000).
23. Petrášek, J., Elčkner, M., Morris, D. A. & Zažímalová, E. Auxin efflux carrier activity and auxin accumulation regulate cell division and polarity in tobacco cells. *Planta* **216,** 302–308 (2002).
24. Petrášek, J. *et al.* Do phytotropins inhibit auxin efflux by impairing vesicle traffic? *Plant Physiol.* **131,** 254–263 (2003).
25. Delarue, M., Muller, P., Bellini, C. & Delbarre, A. Increased auxin efflux in the IAA-overproducing *sur1* mutant of *Arabidopsis thaliana*: a mechanism of reducing auxin levels? *Physiol. Plant.* **107,** 120–127 (1999).
26. Richards, S., Hillman, T. & Stern, M. Mutations in the *Drosophila* pushover gene confer increased neuronal excitability and spontaneous synaptic vesicle fusion. *Genetics* **142,** 1215–1223 (1996).
27. Cutler, S., Ehrhardt, D., Griffitts, J. & Somerville, C. Random GFP::cDNA fusions enable visualisation of subcellular structures in cells of *Arabidopsis* at a high frequency. *Proc. Natl Acad. Sci. USA* **97,** 3718–3723 (2000).
28. Friml, J., Benková, E., Mayer, U., Palme, K. & Muster, G. Automated whole-mount localization techniques for plant seedlings. *Plant J.* **34,** 115–124 (2003).
29. Friml, J. *et al.* AtPIN4 mediates sink-driven auxin gradients and root patterning in *Arabidopsis*. *Cell* **108,** 661–673 (2002).
30. Pimpl, P. *et al.* In situ localization and *in vitro* induction of plant COPI -coated vesicles. *Plant Cell* **12,** 2219–2236 (2000).

Supplementary Information is linked to the online version of the paper at www.nature.com/nature.

Acknowledgements We thank C. Bellini, M. Bennett, M. Estelle, M. Grebe, W. Michalke, D. Robinson and Y. Zhao for sharing material, and E. Benková, P. Brewer, J. Eder, J. Malbeck, C. Oecking, M. Sauer, H. Stransky and D. Weijers for technical assistance and discussions. This work was supported by the Volkswagenstiftung (J.F. and T.P.), the F. Ebert Stiftung (J.K.-V.), the Deutsche Forschungsgemeinschaft (N.G., G.J. and Y.-D. S.), the Grant Agency of the Academy of Sciences of the Czech Republic (J.P. and E.Z.) and the Royal Society of London (D.A.M.).

Author Information Reprints and permissions information is available at npg.nature.com/reprintsandpermissions. The authors declare no competing financial interests. Correspondence and requests for materials should be addressed to J.F. (jiri.friml@zmbp.uni-tuebingen.de).